NASA Technical Memorandum 102110

Acoustic Propagation in Curved Ducts With Extended Reacting Wall Treatment

Kenneth J. Baumeister
Lewis Research Center
Cleveland, Ohio

Prepared for the
1989 Winter Annual Meeting of the
American Society of Mechanical Engineers
San Francisco, California, December 10–15, 1989

NASA

ACOUSTIC PROPAGATION IN CURVED DUCTS WITH EXTENDED REACTING WALL TREATMENT

Kenneth J. Baumeister
National Aeronautics and Space Administration
Lewis Research Center
Cleveland, Ohio 44135

ABSTRACT

A finite-element Galerkin formulation has been employed to study the attenuation of acoustic waves propagating in two-dimensional S-curved ducts with absorbing walls without a mean flow. The reflection and transmission at the entrance and the exit of a curved duct were determined by coupling the finite-element solutions in the curved duct to the eigenfunctions of an infinite, uniform, hard wall duct. In the frequency range where the duct height and acoustic wave length are nearly equal, the effects of duct length, curvature (duct offset) and absorber thickness were examined. For a given offset in the curved duct, the length of the S-duct was found to significantly affect both the absorptive and reflective characteristics of the duct. A means of reducing the number of elements in the absorber region was also presented. In addition, for a curved duct, power attenuation contours were examined to determine conditions for maximum acoustic power absorption. Again, wall curvature was found to significantly effect the optimization process.

INTRODUCTION

Acoustic propagation in duct bends or elbows in the absence of flow or with low Mach number flows plays an important role in industrial ventilation systems and other special applications such as propagation into an ear cavity. Rostafinski (1972 and 1976), Lippert (1954 and 1955), Miles (1947), Cummings (1974), Cabelli (1980), Filler and Blies (1978), Osborne (1976) and von Said (1975) have examined various theoretical and experimental aspects of acoustic propagation in curved ducts without flow. In sound absorbing ducts, the absorptive characteristics of lined curved ducts and lined straight ducts have been modeled by applying the classical admittance boundary conditions at the duct walls. The present investigation will broaden these previous studies of curved ducts to include absorption in extended reaction wall linings where the sound can move axially through the lining parallel with propagation in the main duct.

In a locally reacting liner, such as a Helmholtz resonator array behind a perforated plate, the sound energy interacts normally to the liner and depends only on the local value of acoustic pressure in the adjacent acoustic field. In contrast, the extended reaction liner permits wave propagation in the axial direction, as shown in Fig. 1, and its attenuation characteristics depends on the entire acoustic field. Baumeister and Dahl (1987 and 1989) developed a finite-element model to study wave propagation in bulk materials as well as in any heterogeneous medium. The absorptive characteristics of the bulk materials used in those studies relied on the semitheoretical development presented by Hersh (1980). The propagation theory and property formulas were validated by a number of experiments one of which is displayed in Fig. 2. As seen in the upper schematic drawing, a section of bulk absorbing treatment has been placed on the upper surface of the air duct so that acoustic energy can be absorbed. The plane acoustic wave represented by the vertical line in the entrance of the straight duct will pass under the bulk absorber and be partially absorbed. Figure 2 illustrates the typical agreement between the predictions and the experimental results for the decrease in root-mean-square pressure.

In the present paper, this finite-element model will be used to study wave propagation in curved S-shaped ducts with absorbing walls. This paper will focus on the interaction of a plane wave traveling down the uniform entrance duct with the curved walls as shown in Fig. 3. In the frequency range where the duct height and acoustic wavelength are nearly equal, the effects of duct length, curvature (duct offset) and absorber thickness on wall absorption will now be examined. A means of reducing the number of elements in the absorber region will also be presented. In addition, power attenuation contours will be examined to determine conditions for maximum acoustic power absorption.

NOMENCLATURE

A property term, Eq. (9)

B property term, Eq. (10)

b' characteristic duct height

b_a dimensionless entrance height, b'_a/b'

c'_o adiabatic speed of sound

E acoustic power

f dimensionless frequency, $f'b'_a/c'_{oa} = b'_a/\lambda'_{oa}$

h dimensionless duct offset height, h'/b'_a

i $\sqrt{-1}$

L dimensionless length, $L'b'_a$

N_x grid points in the axial direction

$\bar{n}$ outward unit normal

P dimensionless acoustic pressure, $P'(x,y,t)/\rho'_{oa}c'^2_{oa}$

p dimensionless pressure, $P(x,y,t)/e^{i\omega t}$

T dimensionless thickness of absorber wall, T'/b'_a

t dimensionless time, $t'c'_{oa}/b'_a$

x dimensionless axial distance, x'/b'_a

y dimensionless transverse distance, y'/b'_a

α dimensionless attenuation constant, Eq. (7)

ß dimensionless phase constant, Eq. (8)

ε dimensionless complex property constant

λ dimensionless wavelength

μ dimensionless complex property constant

ρ_o dimensionless density, ρ'_o/ρ'_{oa}

ω dimensionless angular velocity, $\omega'b'_a/c'_o$

ω' angular velocity, $2\pi f'$

Subscripts:

a inlet duct condition

o ambient condition

x x-component

y y-component

Superscripts:

' dimensional quantity

R real part

I imaginary part

GEOMETRIC MODEL

Again consider the idealized acoustic duct shown in Fig. 3 which can be used to simulate acoustic wave propagation in a rectangular two-dimensional curved duct in the absence of flow. The interior passage is assumed to contain air while an acoustic absorber is mounted in the cavity above and below the duct in the central portion.

In the finite-element modeling of the central region, an S-shaped has been chosen to approximate the two-dimensional cross-sectional profile that might be found in a typical bend, as shown in Fig. 3. The S-shaped profile can be prescribed by a simple third-degree polynomial of the form

$$y = h\left[3\left(\frac{x}{L}\right)^2 - 2\left(\frac{x}{L}\right)^3\right] \qquad (1)$$

where the dimensionless duct coordinates are defined as

$$y = \frac{y'}{b'_a} \qquad x = \frac{x'}{b'_a} \qquad h = \frac{h'}{b'_a} \qquad L = \frac{L'}{b'_a} \qquad (2)$$

and b'_a is the dimensional height of the straight duct leading into the curved duct and h is the dimensionless offset height of the duct. The S-curve defined by Eq. (1) has zero slope at x/L of 0 and 1; providing a smooth transition from a straight entrance to the curved test section. In the foregoing equations, the prime is used to denote a dimensional quantity and the unprimed symbols define a dimensionless quantity. This convention will be used throughout this paper. These and all other symbols used in the paper are defined in the nomenclature.

Some sort of acoustic pressure disturbance is assumed to generate a harmonic pressure field at minus infinity in the entrance duct. This field will propagate down the duct and act as the input driving boundary condition for the problem. A positive going acoustic wave of known magnitude is assumed at the entrance (x = 0.0) of the finite-element portion of the duct. The pressure wave may be plane or have significant transverse y pressure variations. The present paper will focus on the interaction of plane propagating acoustic waves with the extended reaction absorbing materials.

In the uniform, infinitely long, entrance and exit duct regions with perfectly hard walls, the exact solution of the governing differential equations can be easily written in terms of the duct modes (Astley and Eversman 1981); thus, simple analytical expressions can be employed to describe the pressure field in these regions. In the central region which includes both the duct and the absorber region, the finite-element analysis is employed to determine the pressure field.

The assumed known pressure waves propagating down the hard wall entrance duct are partially reflected, transmitted and absorbed by the nonuniform segment of the duct containing the acoustic absorber. Pressure mode reflection at the inlet to the absorbing region and transmission at the outlet of the absorbing region are determined by matching the finite-element solution in the interior of the central region to the known analytical eigenfunction expansions in the uniform inlet and exit ducts. This permits a multimodal representation accounting for reflection and mode conversion by the nonuniform absorbing section (Astley and Eversman 1981). This approach has been found to accurately model reflection and transmission coefficients (Baumeister et al. 1983).

GOVERNING EQUATION AND BOUNDARY CONDITIONS

The acoustic propagation through the two-dimensional Cartesian duct and absorber regions in Fig. 3. can be modeled by solutions of the continuity, momentum, and state linearized gas dynamic equations in the absence of flow. As developed by Baumeister and Dahl (1987), for harmonic pressure propagation ($e^{+i\omega t}$) in the heterogeneous absorber material, the equations

of state, continuity, and momentum were combined to yield the following wave equation in dimensionless form:

$$\frac{\delta}{\delta y}\left(\frac{1}{\varepsilon_y}\frac{\delta P}{\delta y}\right) + \frac{\delta}{\delta x}\left(\frac{1}{\varepsilon_x}\frac{\delta P}{\delta x}\right) + \omega^2 \mu p = 0 \qquad (3)$$

The usual symbols for acoustic propagation are employed and all are explicitly defined in the nomenclature.

The relationship between ε and μ and the physical properties of the medium is complicated. For propagation in air, ε equals the fluid density and μ is the inverse of the product of density and the speed of sound squared. For bulk absorbers, Baumeister and Dahl (1987, Eqs. (25) to (27)) employed Hersh's model (1980) in explicitly relating ε and μ to the porosity, a viscous loss coefficient, a heat transfer parameter and an effective speed of sound of the medium. Morse and Ingard (1968, p. 253) also developed more general parameters for describing propagation in porous media for which ε and μ can be related.

In the present paper, the parameters ε and μ will be treated as mathematical quantities independent of property correlations. In particular, the values of ε and μ associated with the optimum absorption properties will be examined.

At the hard walls shown by the dark thick lines in Fig. 3, the acoustic velocity normal to the wall is zero. Again, using the momentum equations to relate the acoustic velocity to the pressure fields requires

$$\nabla p \cdot \bar{n} = 0 \qquad (4)$$

In addition, recall that a model solution (Morse and Ingard 1968, p. 504) is used to represent the pressure in the semi-infinite, hard wall entrance and exit regions while a finite-element solution is used to generate the solution in the curved portion of the duct. Consequently, both pressure and velocity continuity are required of the modal and finite-element solutions at the entrance and exit interfaces separating the finite-element and modal regions. This is easily enforced as discussed by Astley and Eversman (1981).

Finally, it is not necessary to employ any interfacial boundary condition inside the finite-element region. For example the thin black line in Fig. 3 separating the air duct from the absorber region requires no special consideration. The heterogeneous form of the wave equation (Eq. (3)) automatically handles the change in properties (Baumeister and Dahl 1989, Fig. 7).

FINITE-ELEMENT THEORY

In the central portion of the duct containing the curved region, the continuous domain is first divided into a number of discrete areas as shown in Fig. 3. In the classical weighted residual manner, the pressure field is curve-fitted in terms of all the unknown nodal values $p_i(x_i, y_i)$. The finite-element aspects of converting Eq. (3) and the boundary conditions into an appropriate set of global difference equations can be found in textbooks (Burnett 1987) or more explicitly in the paper by Baumeister (1986) and for conciseness will not be presented herein.

RESULTS AND COMPARISONS

A number of example calculations are now presented to illustrate the use of the finite-element theory as applied to curved ducts with extended reaction absorbing walls. First, typical duct geometries and element arrangements used in the numerical examples are discussed. Next, the effects of offset and duct length on the transmitted acoustic energy are examined for a fixed wall absorption layer. Then, the effect of absorber thickness is considered. To reduce storage requirements, the element spacing requirements in the absorber material are examined. Finally, the power attenuation contours for a curved duct which maximizes the input signal absorption are examined.

Duct Geometry

The grid generation package generates the geometries and the linear triangular finite-element grid shown in Fig. 4, for a typical straight duct (Fig. 4(a)) and curved duct with maximum offset (h = 1, Fig. 4(b)). The absorber has been placed above and below the ducts. All of the curved duct geometries are of the form shown but with different lengths, offsets and absorber thickness.

Example 1: Transmitted Power

The effect of duct curvature and length on transmitted power in a duct are examined in Fig. 5 for various values of duct offset. The geometrical configuration is shown by the sketch inserted in Fig. 5. In this case, the entrance and exit ducts stretch from minus infinity to plus infinity which signifies the absence of reflected energy at the exit termination.

The wall properties were taken to be $\varepsilon_w = 1.0 - i\,2.83$ and $\mu_w = 4.1$. These properties are associated with nearly maximum absorption of a plane pressure wave in a straight duct at the frequency of unity, as will later be examined in Ex. 4. For a fixed length of duct, as seen in Figs. 5(a), (b), and (c), an increase in the duct offset parameter h increases the attenuation of the transmitted acoustic power (integral of the product of pressure, acoustic velocity and cross-sectional area) at the exit of the curved lined portion. This effect is most pronounced for the smaller duct lengths as shown in Figs. 5(a) and (b). The root-mean-square pressure fields inside the duct are illustrated in Fig. 6 for the duct with 0.75 length. As seen in Fig. 6(a) the pressure remains high in the central portion of the duct with grazing contact along the absorbing wall until it reaches the exit with very little attenuation. In contrast, in Fig. 6(e) the pressure field comes in nearly normal contact with the wall and quickly dies out giving rise to the much larger power attenuation shown in Fig. 5(a).

Example 2: Absorber Thickness

In this section the effect of absorber thickness is briefly examined. The configuration considered is again shown by the sketch in the upper portion of Fig. 7. In this case the duct length and offset will be held fixed at unity, the wall properties held at the value of the previous example, and the wall absorber thickness will be varied. As seen in Fig. 7 for thickness of 0.1 or greater, the power variation along the axial length of the duct remains similar in shape and about the same magnitude. Clearly, only the absorber layer immediately adjacent to the surface contributes to the absorption of the acoustic energy. For thickness of 0.05 and 0.01 significant decreases in the energy absorbed are seen.

Example 3: Axial Discretization in Wall Absorber

For linear elements employed in finite-element solutions of the wave equation, roughly 12 grid points per wavelength of the dependent variable are required to accurately resolve the complex pressure field and the transmitted or reflected acoustic power. In performing finite-element calculations, the number of axial nodal points should be held to a minimum to reduce computer storage as well as solution time. This

is especially true in calculations with large values of the wall properties ε and μ which lead to very small wavelengths in the material. The wave length for plane wave propagation in lossy material will now be determined from a solution of the wave equation and a strategy for reducing computer storage will be presented.

For plane waves propagating in a homogeneous lossy material, Eq. (3) reduces to

$$\frac{\delta}{\delta x}\left(\frac{\delta p}{\delta x}\right) + \omega^2 \varepsilon \mu p = 0 \tag{5}$$

The solution of which can be written as

$$p = e^{-\alpha x}\, e^{-i\beta x} \tag{6}$$

where

$$\alpha = \frac{\omega}{\sqrt{2}}\left(\sqrt{A^2 + B^2} - B\right)^{1/2} \tag{7}$$

$$\beta = \frac{1}{\sqrt{2}}\left(\sqrt{A^2 + B^2} + B\right)^{1/2} \tag{8}$$

$$A = \varepsilon^I \mu^R + \varepsilon^R \mu^I \tag{9}$$

$$B = \varepsilon^R \mu^R - \varepsilon^I \mu^I \tag{10}$$

The superscripts R and I stand for real and imaginary parts and the wavelength can be expressed in terms of the propagation phase constant β as follows:

$$\lambda = \frac{2\pi}{\beta} \tag{11}$$

The number of grid points N_x in the axial direction to accurately resolve the acoustic field is

$$N_x = \frac{12L}{\lambda} = \frac{6\beta L}{\pi} \tag{12}$$

For the special case where the duct length is just equal to the axial wavelength of the acoustic wave, 12 nodal points are required in the axial direction. If the duct length is twice the wavelength then 24 nodes would be required. Thus the number of nodes is just 12 times the duct length to wavelength ratio.

For large values of ε and μ associated with wall absorbers, the phase constant β increases according to Eq. (8) which leads to smaller values of the wavelength according to Eq. (11) and a considerably larger number of axial nodes according to Eq. (12). However, a plane wave incident obliquely at an interface with an absorbing medium will generally be bent toward the normal (Reynolds 1981, p. 298 and Attenborough 1982, p. 210) making the energy transfer in the wall absorber normal to the direction of the energy transfer in the duct itself and thereby partially reducing the axial energy transfer in the wall absorber. Since the axial attenuation in the duct wall will be much larger than in the air duct, consideration is now given to basing the axial grid spacing on the wavelength of the air duct rather than the wall absorber wavelength. In this case the axial grid point spacing would be

$$N_x = \frac{12L}{\lambda_{air}} = 12Lf \tag{13}$$

If such an approximation is valid, large savings in computer storage are possible.

The validity of Eq. (13) in predicting acoustic power attenuations and pressure fields is now examined for two extremes of wall properties. First the moderate value listed in Fig. 8(a) and then the much larger value listed in Fig. 8(b). As seen in the upper portion of Fig. 8(a), axial spacing based on the wall properties using Eq. (12) results in a much denser grid than the lower figure based on the wavelength in air using Eq. (13). For the large wall property value, the grid density is even greater as seen in the upper portion of Fig. 8(b).

For the duct configuration shown in the upper portion of Fig. 9, exact calculations for duct attenuation displayed in Fig. 9 indicate that the axial spacing based on air properties (Eq. (13)) gives nearly the same results for duct attenuation as the axial spacing based on the wall material (Eq. (12)). The attenuation in dB on the ordinate in Fig. 9 is defined by

$$dB = 10 \log_{10}\left(\frac{E}{E_o}\right) \tag{14}$$

where E is the total axial power at the exit and E_o the power at the entrance.

In addition, the contour plots of the pressure field inside the air duct (Figs. 10(a) and (b)) show that the pressure field in the duct is for all practical purposes identical when either Eq. (12) or (13) is employed to set the axial grid point density.

Finally, the sensitivity to the number of transverse nodes in the wall absorber is determined in Fig. 11. As seen in Fig. 11 only five transverse nodes are required to accurately estimate the attenuation in a 0.1-thick absorber coating with the same range of property variations previously considered.

Example 4: Attenuation Contours

Optimizing the wall absorber for maximum attenuation can be an important part of the design of an acoustic duct suppressor. In duct acoustics employing local impedance boundary conditions, the maximum possible attenuation occurs at the so-called optimum impedance. For a particular acoustic mode or more generally for modes with common cut-off ratios, the optimum impedance can be determined analytical from semi-infinite duct theory using a single soft-wall mode (Rice 1979). Unruh (1976) has determined the optimum impedance for finite-length liners.

Consider a plane wave propagating down a duct, as shown in the upper schematic of Fig. 12. By an iteration process (hold one wall property fixed and varying the other), the attenuation contours were determined throughout the ε plane with increments of 0.5 taken in the real and imaginary parts of ε. The optimum wall value associated with maximum signal reduction is seen in Fig. 12 to occur at a ε of 1.5 - i 3.5 with μ equal to 4.1. The magnitude of the imaginary part of ε is shown positive in Fig. 12. The optimum wall ε is represented by the peak contours enclosed in the smallest circle of Fig. 12. The dB contours in Fig. 12 have been normalized between 0 and 1 by the simple expression:

$$\text{contour level} \sim \frac{|dB| - |dB_{min}|}{|dB_{max}| - |dB_{min}|} \tag{15}$$

The maximum attenuation of the incoming wave is 36.5 dB associated with this local optimum point as displayed in Fig. 12.

For the same geometry as considered in Fig. 12, the sensitivity of the initial starting material value on the contours was examined and found to be quite significant. The optimum properties can vary depending on the initial starting value of μ used in the optimum search. In Fig. 12, the ratio of (μ/ϵ) at the optimum point is 0.424 + j 0.989. Performing additional calculations with different starting points, it was found that any combination of material properties with approximately the same ratio of (μ/ϵ) will have yielded similar values of the maximum attenuation. As commonly used in electromagnetic theory, $\sqrt{\mu/\epsilon}$ can be defined as an intrinsic impedance of the wall.

The curvature of the duct will play a significant role in determining the wall materials to obtain the maximum attenuation. For a straight duct (h = 0) of unit length, the optimum intrinsic impedance has shifted to a new value of approximately 0.033 + i 0.373 and the local optimum attenuation has a maximum value of 22.113.

CONCLUDING REMARKS

A finite-element Galerkin formulation was used to study acoustic wave propagation in two-dimensional curved S-shaped ducts with extended reaction absorbing walls. Example solutions illustrated the relationship of absorption on the length, thickness and offset of curved duct absorbing walls and the mesh spacing requirement in highly absorbing materials. Optimum properties to maximize wall absorption were also examined.

For a given wall absorber and fixed liner length, increased offset greatly increases the power attenuation. Furthermore, it was shown that increasing the absorber thickness beyond a specific value will have little affect on the sound power attenuation. Also, the grid spacing in the highly absorbent wall can be the same as in the air duct without loss of accuracy in the numerical solution.

REFERENCES

Astley, R.J., and Eversman, W., 1981, "Acoustic Transmission in Non-Uniform Ducts with Mean Flow, Part II: The Finite Element Method," Journal of Sound and Vibration, Vol. 74, pp. 103-121.

Attenborough, K., 1982, "Acoustical Characteristics of Porous Materials," Physics Reports, Vol. 82, No. 3, pp. 179-227.

Baumeister, K.J., 1986, "Finite Element Analysis of Electromagnetic Propagation in an Absorbing Wave Guide," NASA TM-88866.

Baumeister, K.J., and Dahl, M.D., 1987, "A Finite Element Model for Wave Propagation in an Inhomogeneous Material Including Experimental Validation," AIAA Paper 87-2741, (also NASA TM-100149).

Baumeister, K.J., and Dahl, M.D., 1989, "Acoustic Wave Propagation in Heterogeneous Structures Including Experimental Validation," AIAA Paper 89-1044, (also NASA TM-101486).

Baumeister, K.J., Eversman, W., Astley, R.J., and White, J.W., 1983, "Acoustics in Variable Area Duct: Finite Element and Finite Difference Comparison to Experiment," AIAA Journal, Vol. 21, No. 2, pp. 193-199.

Burnett, D.S., 1987, Finite Element Analysis, Addison-Wesley Publishing Co., Reading, MA.

Cabelli, A., 1980, "The Acoustic Characteristics of Duct Bends," Journal of Sound and Vibration, Vol. 68, pp. 369-388.

Cummings, A., 1974, "Sound Transmission in Curved Duct Bends," Journal of Sound and Vibration, Vol. 35, pp. 451-477.

Fuller, C.R., and Bies, D.A., 1978, "Propagation of Sound in a Curved Bend Containing a Curved Axial Partition," Journal of the Acoustical Society of America, Vol. 63, pp. 681-686.

Hersh, A.S., and Walker, B., 1980, "Acoustic Behavior of Fibrous Bulk Materials," AIAA Paper 80-0986.

Lippert, W.K.R., 1954, "The Measurement of Sound Reflection and Transmission at Right Angle Bends in Rectangular Tubes," Acustica, Vol. 4, pp. 313-319.

Lippert, W.K.R., 1955, "Wave Transmission Around Bends of Different Angles in Rectangular Ducts," Acustica, Vol. 5, pp. 274-277.

Miles, J.W., 1947, "The Diffraction of Sound Due to Right Angled Joints in Rectangular Tubes," Journal of the Acoustical Society of America, Vol. 19, pp. 572-579.

Morse, P.M., and Ingard, K.U., 1968, Theoretical Acoustics, McGraw-Hill, New York.

Osborne, W.C., 1976, "Higher Mode Propagation of Sound in Short Curved Bends of Rectangular Cross Section," Journal of Sound and Vibration, Vol. 45, pp. 39-52.

Reynolds, D.D., 1981, Engineering Principles of Acoustics: Noise and Vibration Control. Allyn and Bacon, Inc., Boston, MA.

Rice, E.J., 1979, "Optimum Wall Impedance for Spinning Modes - a Correlation With Mode Cut-Off Ratio," Journal of Airacraft, Vol. 16, No. 5, pp. 336-343.

Rostafinski, W., 1972, "On Propagation of Long Waves in Curved Ducts," Journal of the Acoustical Society of America, Vol. 52, pp. 1411-1420.

Rostafinski, W., 1974, "Analysis of Propagation of Waves of Acoustic Frequencies in Curved Ducts," Journal of the Acoustical Society of America, Vol. 56, pp. 11-15.

Rostafinski, W., 1976, "Acoustic Systems Containing Curved Duct Sections," Journal of the Acoustical Society of America, Vol. 60, pp. 23-28.

Unruh, J.F., 1976, "Finite Length tuning for Low Frequency Lining Design," Journal of Sound and Vibration, Vol. 45, No. 1, pp. 5-14.

von Said, A., 1975, "Theorie der Schallaubreitung in Kanalen mit Rechtwinkligen Ecken und Verzweigungen," Acustica, Vol. 33, pp. 203-211.

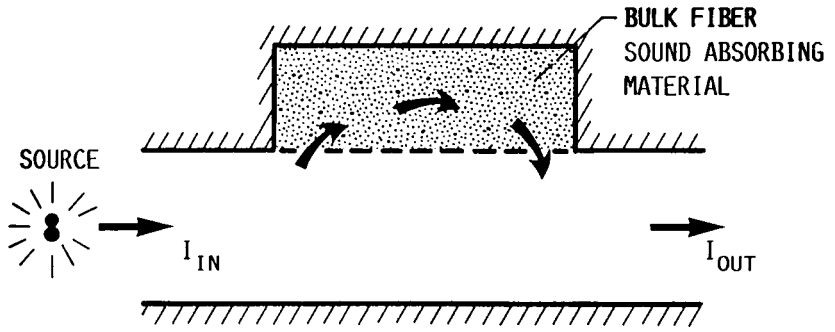

FIGURE 1. - EXTENDED REACTING ABSORBING BOUNDARY.

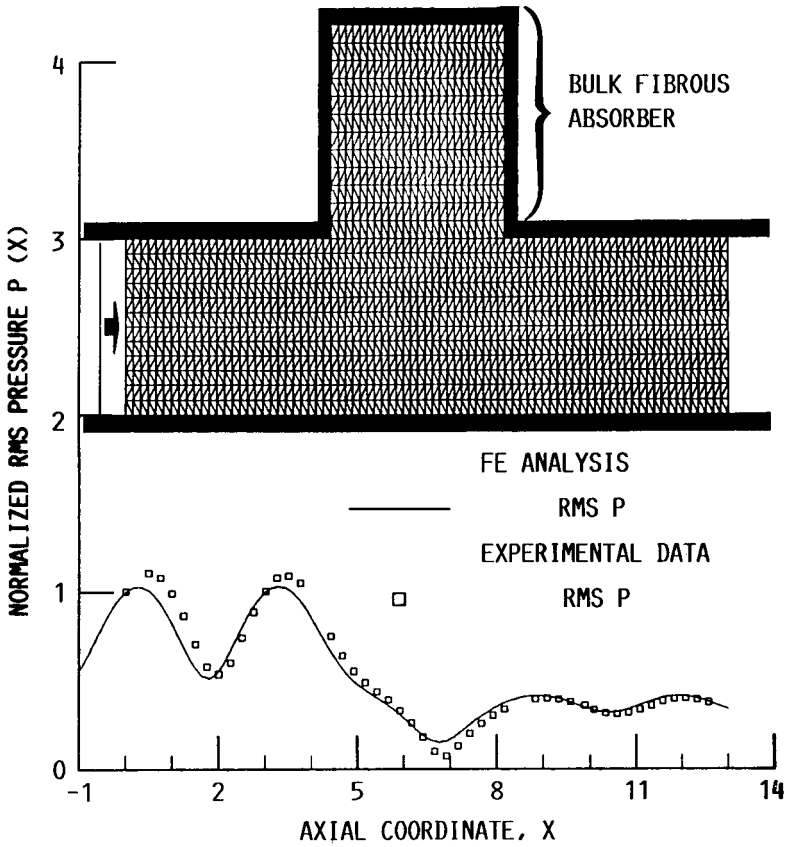

FIGURE 2. - EXPERIMENTAL AND THEORETICAL AXIAL PRESSURE PROFILE ALONG LOWER WALL FOR CAVITY WITH BULK ABSORBER TREATMENT.

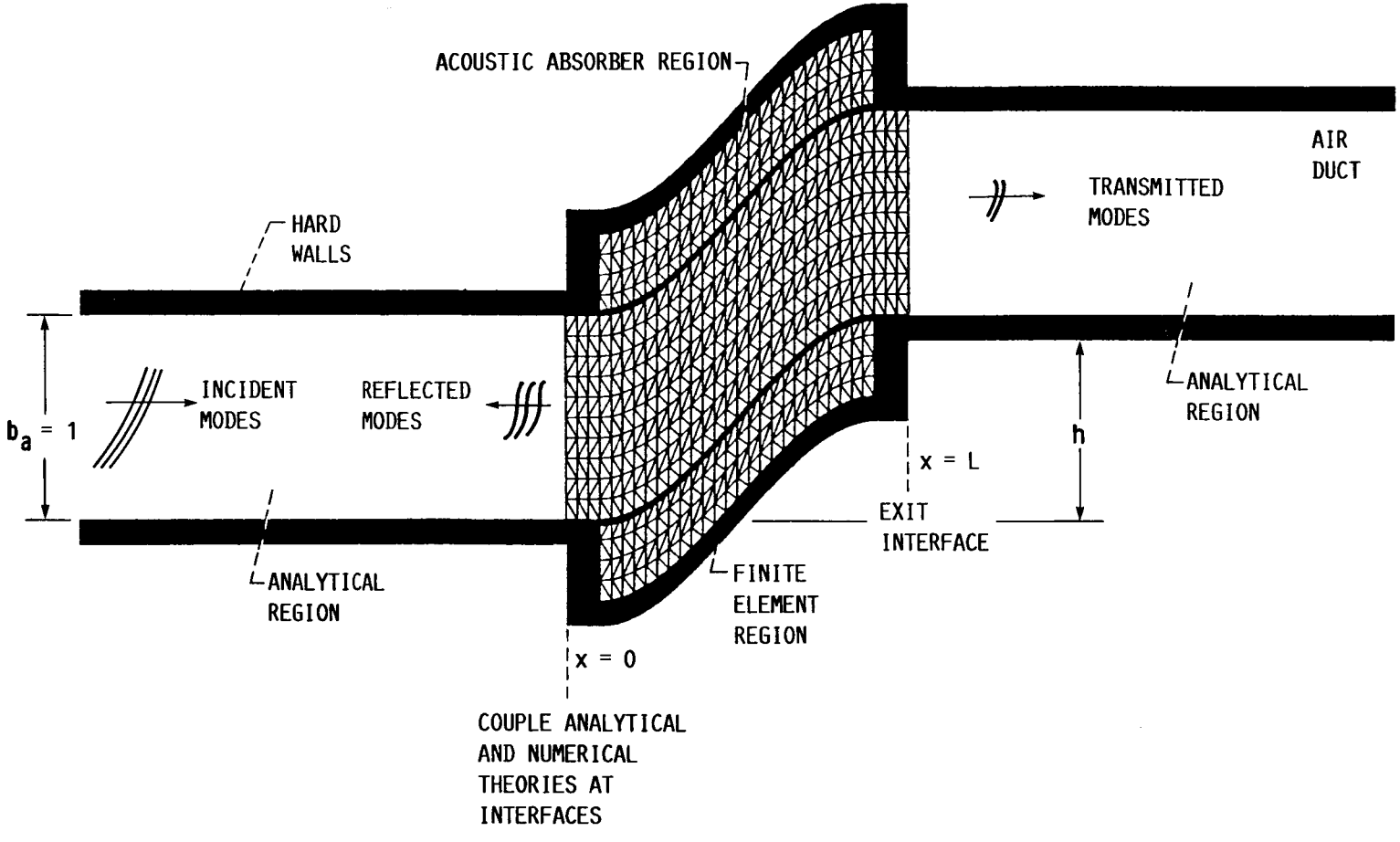

FIGURE 3. - TWO DIMENSIONAL S-DUCT FINITE ELEMENT MODEL.

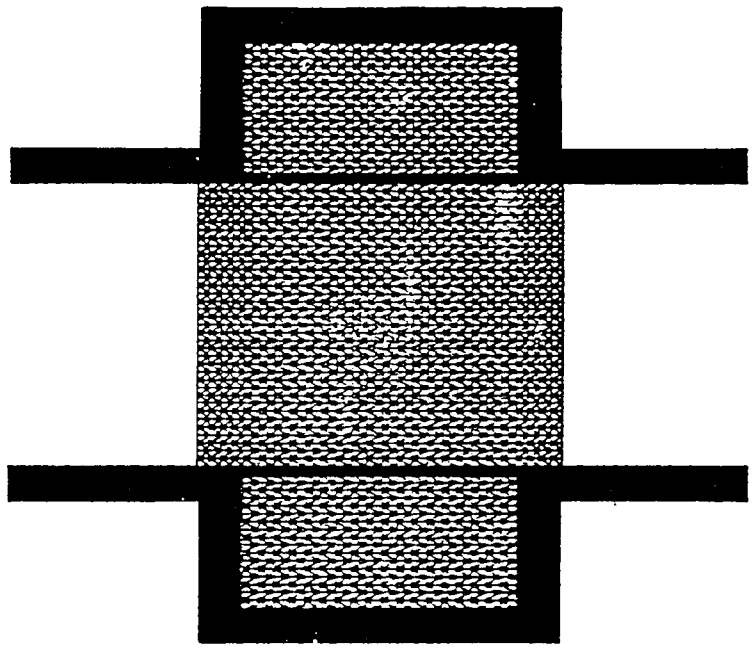

(A) STRAIGHT DUCT.

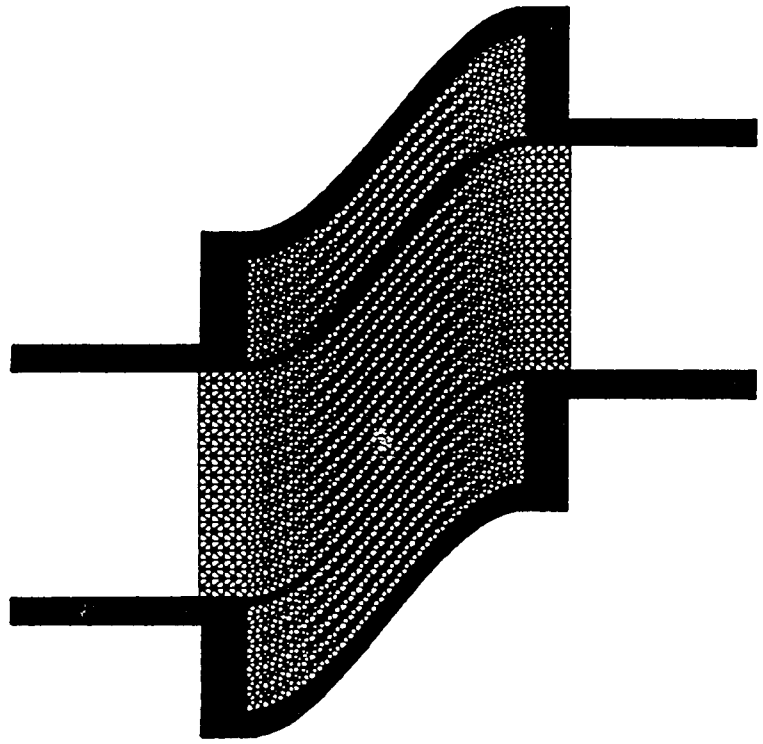

(B) CURVED DUCT.

FIGURE 4. - DISCRETIZATION OF AIR FILLED DUCT WITH ABSORBERS MOUNTED ALONG BOTH UPPER AND LOWER WALLS.

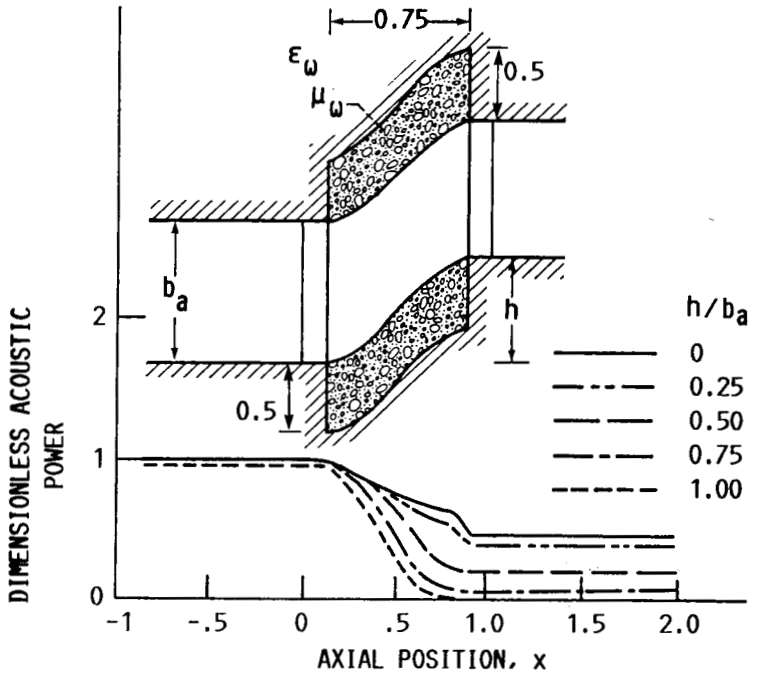

(A) L = 0.75.

FIGURE 5. - EFFECT OF DUCT OFFSET ON THE MAGNITUDE OF THE AXIAL POWER AS A FUNCTION OF POSITION (WALLS $\varepsilon_\omega = 1. - i2.83$; $\mu_\omega = 4.1$ AND f = 1).

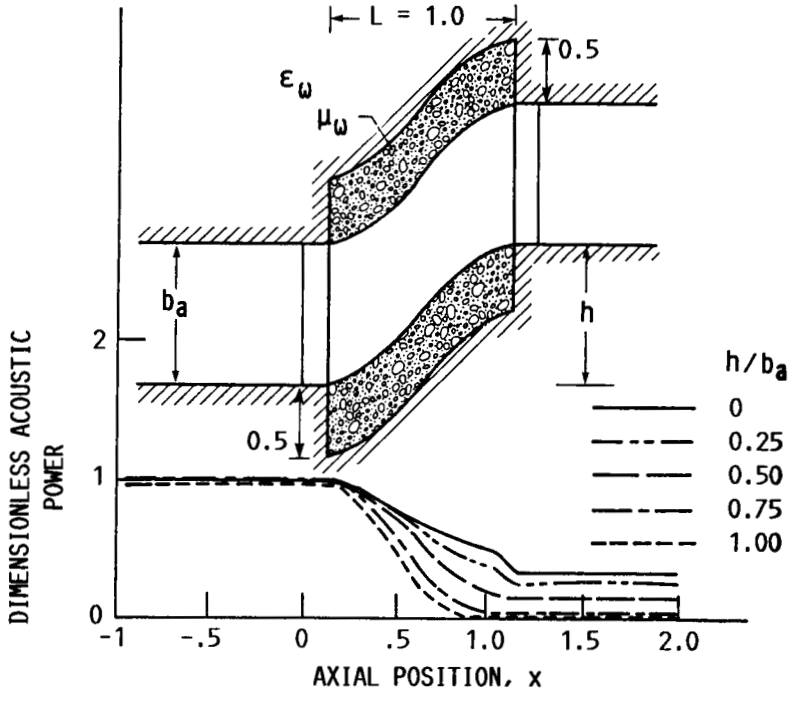

(B) L = 1.0.

FIGURE 5. - CONTINUED.

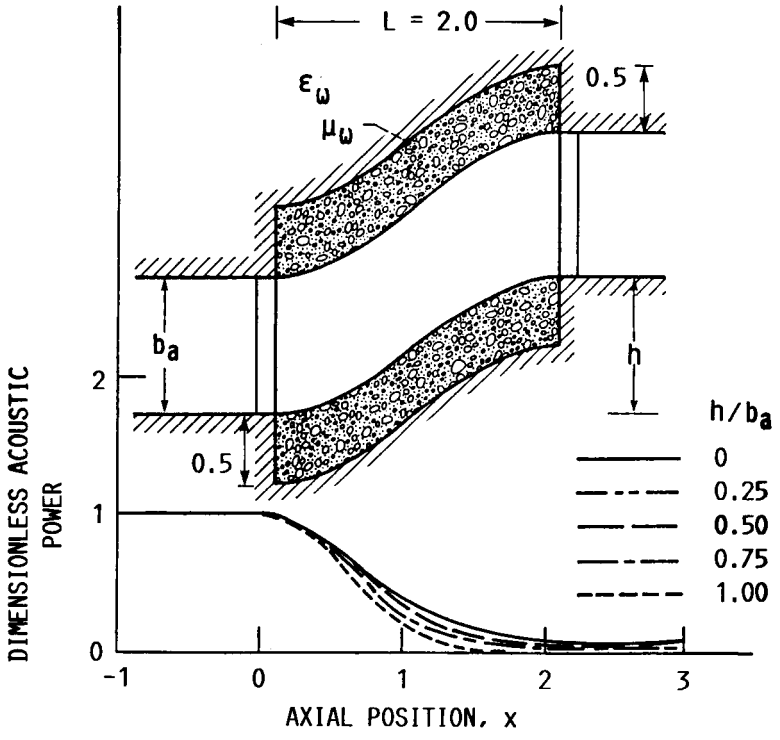

(C) L = 2.

FIGURE 5. - CONCLUDED.

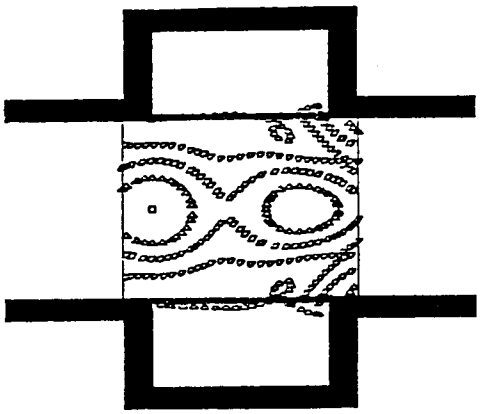

RELATIVE MAGNITUDE

□	1.0
△	.8
▱	.6
▽	.4
○	.2
◇	0

(A) $h/b_a = 0.$

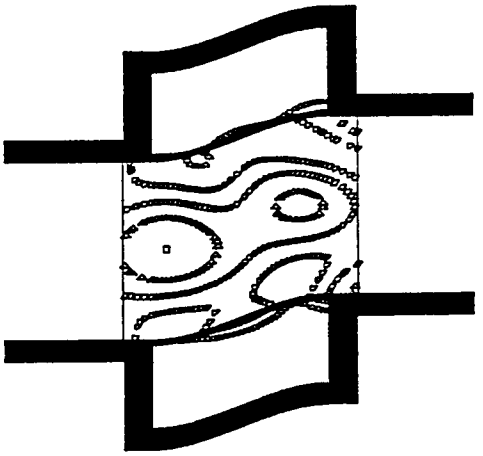

(B) $h/b_a = 0.25.$

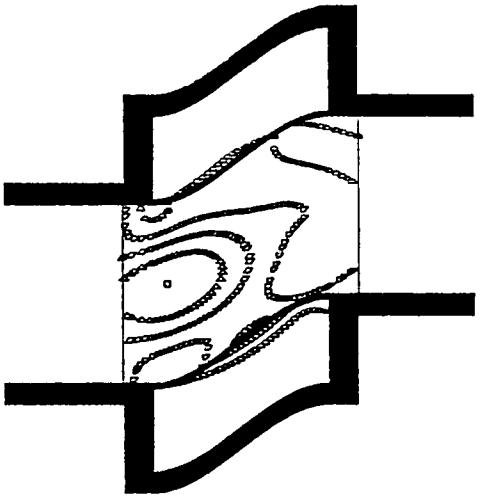

(C) $h/b_a = 0.5.$

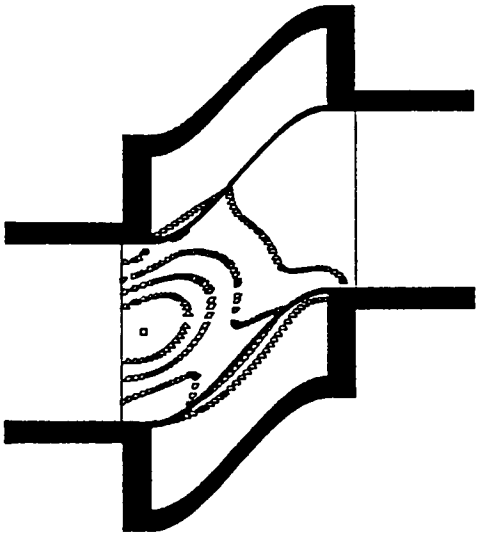

(D) $h/b_a = 0.75.$

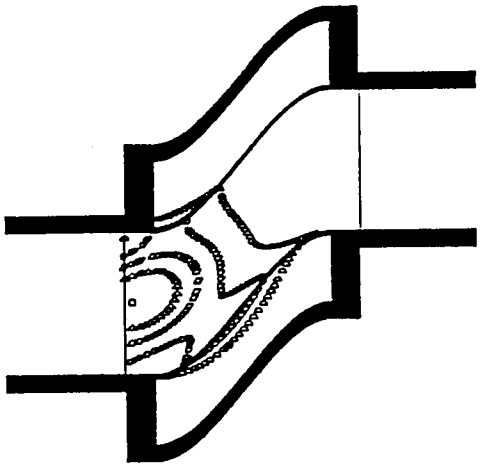

(E) $h/b_a = 1.0.$

FIGURE 6. - EFFECT OF OFFSET OF ABSORBING WALL ON THE CONTOURS OF THE PRESSURE FIELD WITH NONREFLECTING EXIT FOR L = 0.75 AND f = 1.

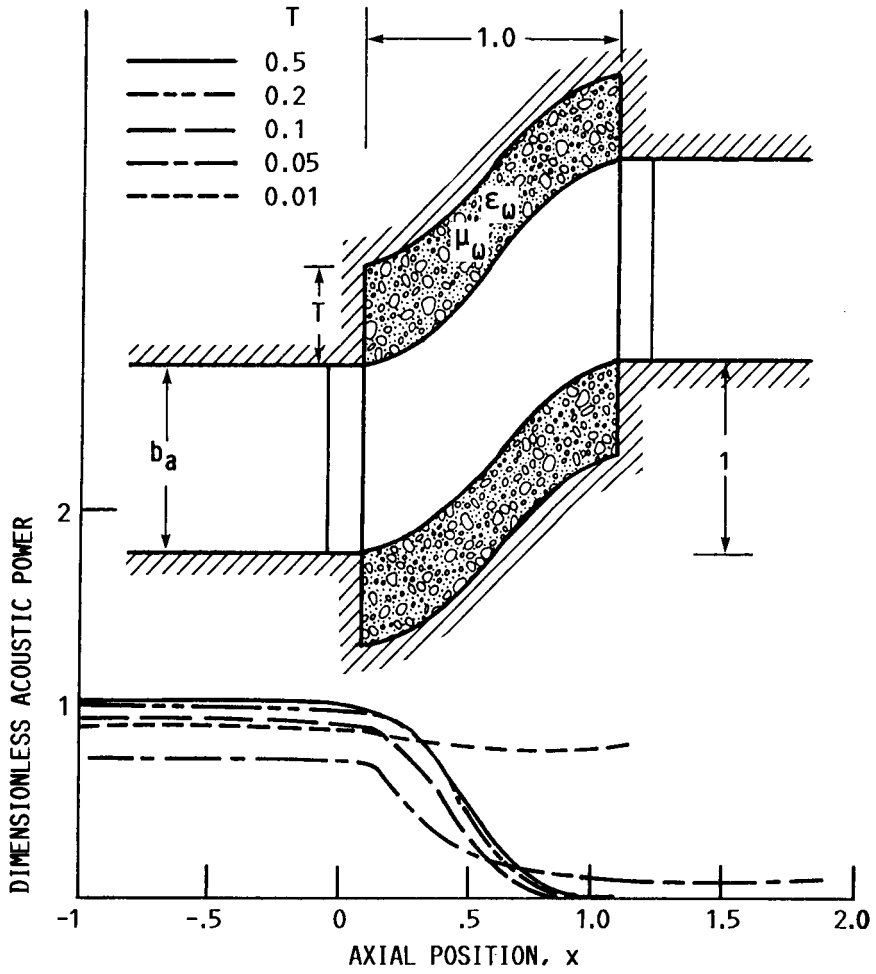

FIGURE 7. - EFFECT OF ABSORBER THICKNESS ON THE MAGNITUDE OF THE AXIAL POWER AS A FUNCTION OF POSITION (ε_ω = 1. - i2.83; μ_ω = 4.1 AND f = 1).

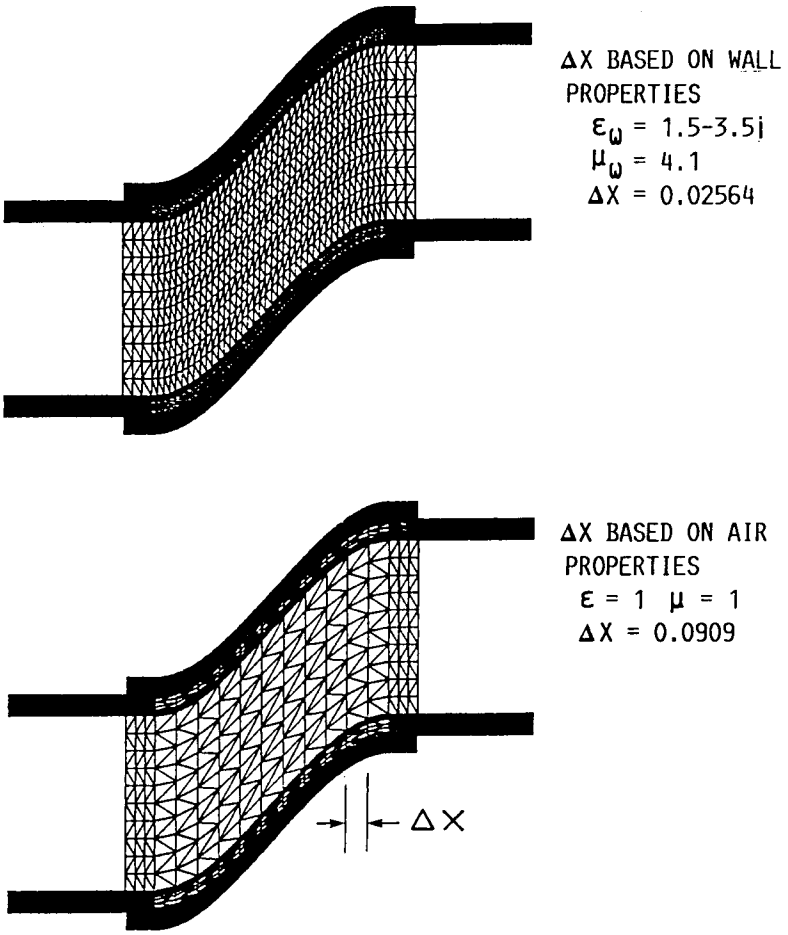

(A) MODERATE CASE ε_ω = 1.5-3.5i.

FIGURE 8. - DISCRETIZATION OF AIR FILLED DUCT WITH ACOUSTIC ABSSORBERS MOUNTED ALONG BOTH UPPER AND LOWER WALLS. (T = 0.1, h = 1, f = 1).

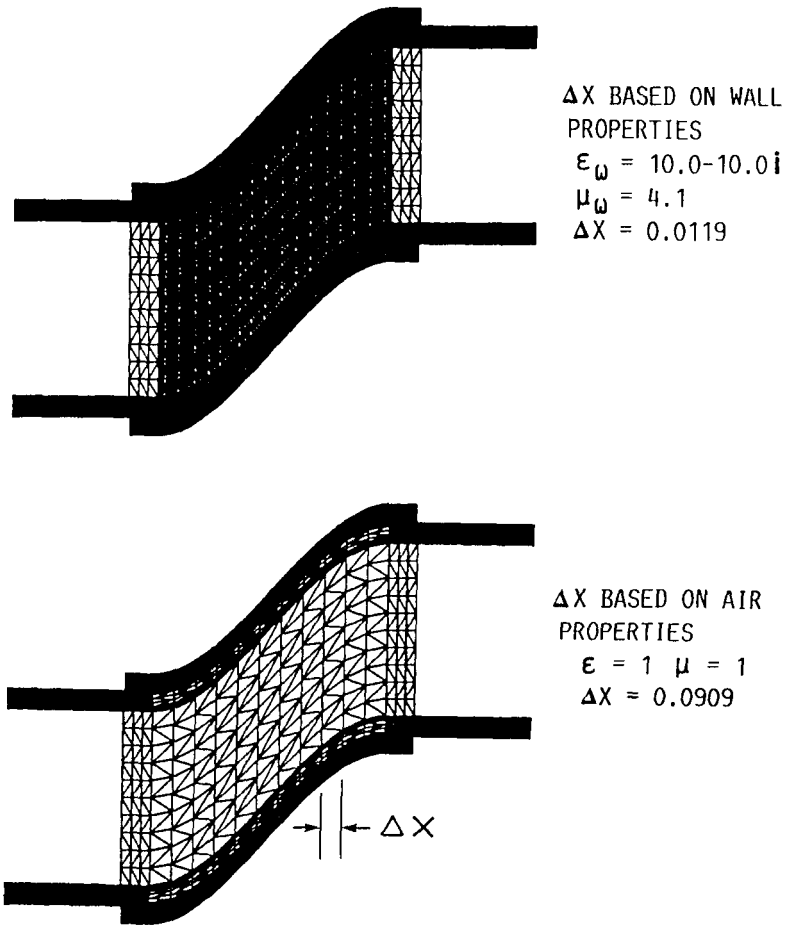

(B) LARGE CASE ε_ω = 10.0-10.0i.

FIGURE 8. - CONCLUDED.

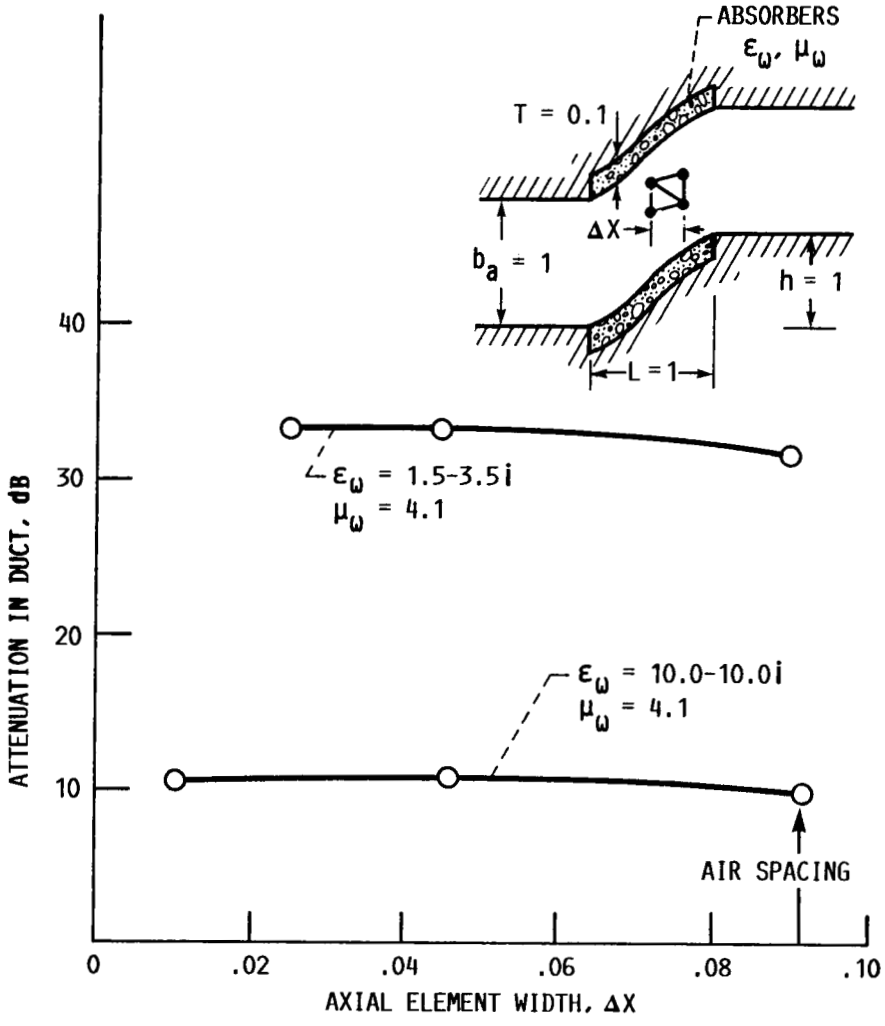

FIGURE 9. - ACOUSTIC POWER ATTENUATION AS A FUNCTION OF AXIAL NODE SPACING IN ABSORBER AND DUCT FOR CURVED DUCTS (f = 1, L = 1, h = 1 WITH 5 VERTICAL NODES IN ABSORBER REGION).

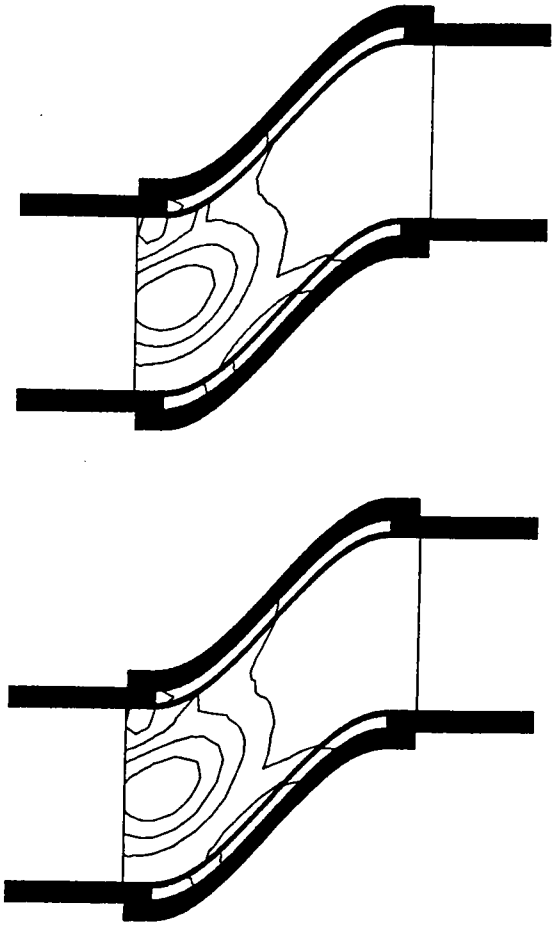

(A) MODERATE CASE ε_ω = 1.5-3.5i μ_ω = 4.1.

FIGURE 10. - CONTOUR PLOTS OF PRESSURE FIELD AMPLITUDE.

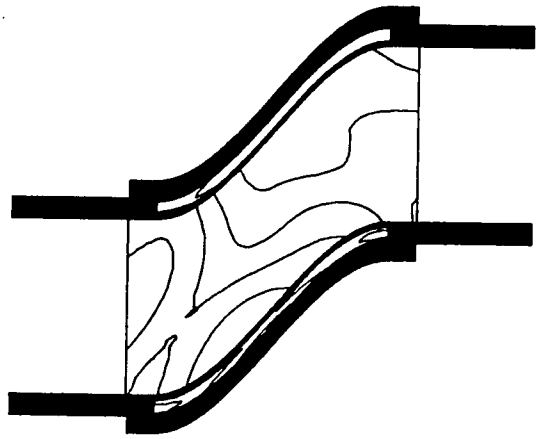

ΔX = 0.0119
BASED ON WALL
PROPERTIES
ε_ω = 10.0-10.0i
μ_ω = 4.1

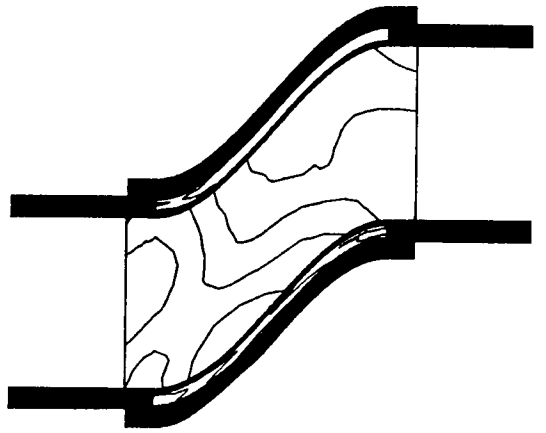

ΔX = 0.0909
BASED ON AIR
PROPERTIES

(B) LARGE CASE ε_ω = 10.0-10.0i μ_ω = 4.1.

FIGURE 10. - CONCLUDED.

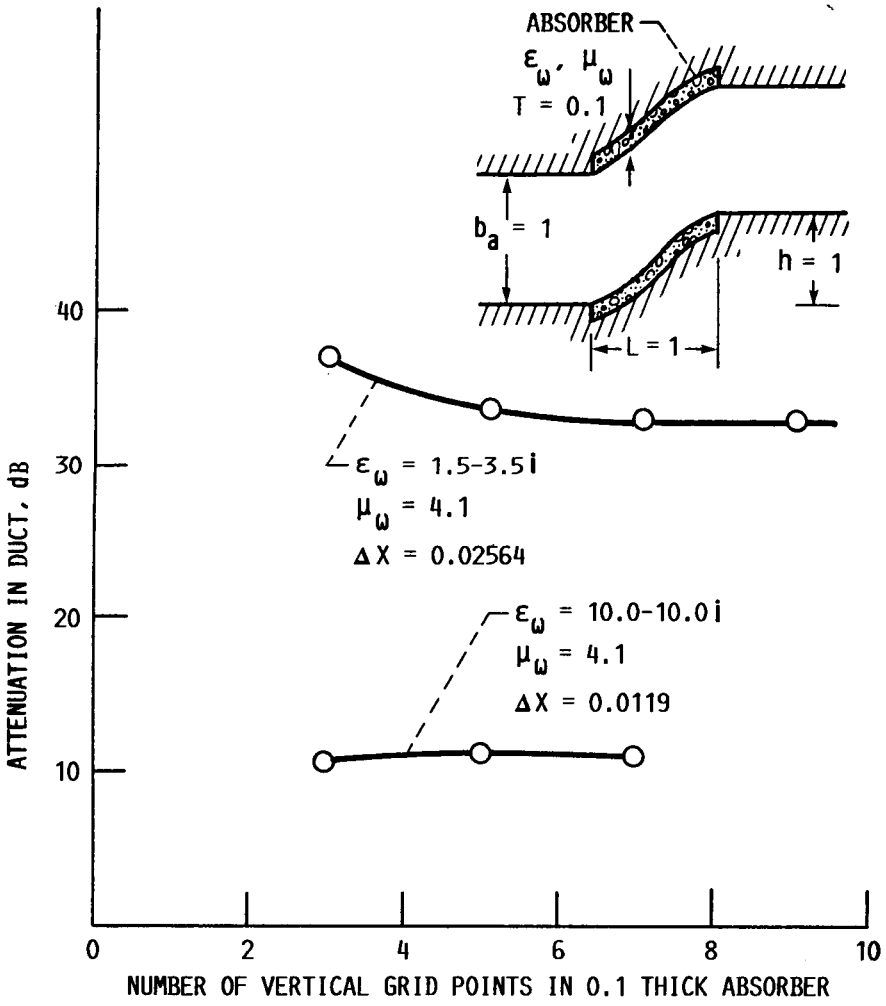

FIGURE 11. - ACOUSTIC ATTENUATION AS A FUNCTION OF VERTICAL NODES IN ABSORBER FOR CURVED DUCT (f = 1, L = 1, h = 1).

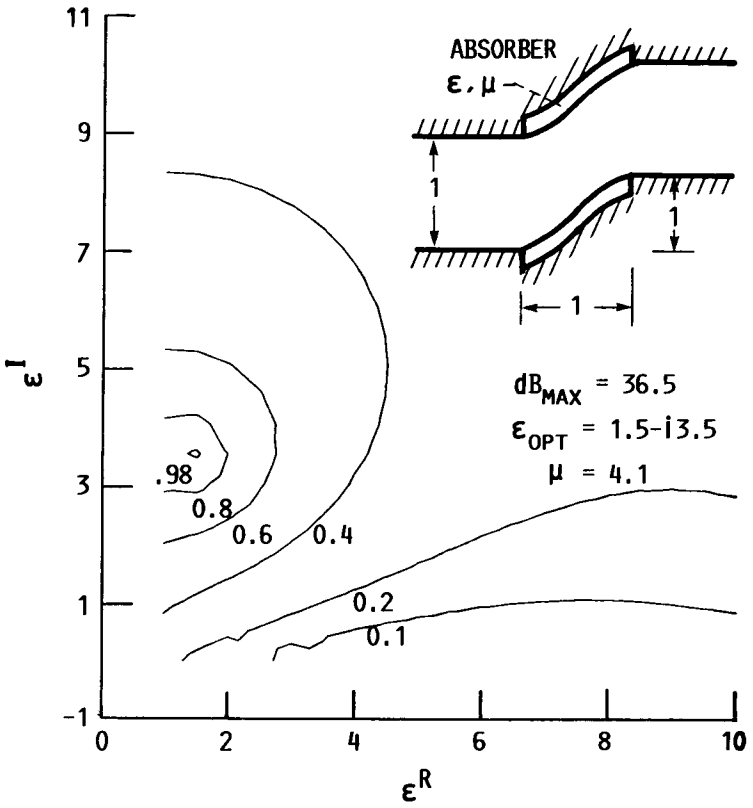

FIGURE 12. - NORMALIZED ACOUSTIC ATTENUATION CONTOURS FOR CURVED DUCT (f = 1, L = 1, h = 1).

NASA
National Aeronautics and Space Administration

Report Documentation Page

1. Report No.	2. Government Accession No.	3. Recipient's Catalog No.
NASA TM-102110		

4. Title and Subtitle	5. Report Date
Acoustic Propagation in Curved Ducts With Extended Reacting Wall Treatment	6. Performing Organization Code

7. Author(s)	8. Performing Organization Report No.
Kenneth J. Baumeister	E-4880
	10. Work Unit No. 505-62-21

9. Performing Organization Name and Address	11. Contract or Grant No.
National Aeronautics and Space Administration Lewis Research Center Cleveland, Ohio 44135-3191	13. Type of Report and Period Covered Technical Memorandum

12. Sponsoring Agency Name and Address	14. Sponsoring Agency Code
National Aeronautics and Space Administration Washington, D.C. 20546-0001	

15. Supplementary Notes

Prepared for the 1989 Winter Annual Meeting of the American Society of Mechanical Engineers, San Francisco, California, December 10-15, 1989.

16. Abstract

A finite-element Galerkin formulation has been employed to study the attenuation of acoustic waves propagating in two-dimensional S-curved ducts with absorbing walls without a mean flow. The reflection and transmission at the entrance and the exit of a curved duct were determined by coupling the finite-element solutions in the curved duct to the eigenfunctions of an infinite, uniform, hard wall duct. In the frequency range where the duct height and acoustic wave length are nearly equal, the effects of duct length, curvature (duct offset) and absorber thickness were examined. For a given offset in the curved duct, the length of the S-duct was found to significantly affect both the absorptive and reflective characteristics of the duct. A means of reducing the number of elements in the absorber region was also presented. In addition, for a curved duct, power attenuation contours were examined to determine conditions for maximum acoustic power absorption. Again, wall curvature was found to significantly effect the optimization process.

17. Key Words (Suggested by Author(s))	18. Distribution Statement
Finite element Acoustics Bulk absorbers Curved duct	Unclassified - Unlimited Subject Category 70

19. Security Classif. (of this report)	20. Security Classif. (of this page)	21. No of pages	22. Price*
Unclassified	Unclassified	14	A03

*For sale by the National Technical Information Service, Springfield, Virginia 22161